Piperlongumine induces apoptosis and G_2/M phase arrest in human osteosarcoma cells by regulating ROS/PI3K/Akt pathway

Jinfeng Zhou[a,1], Zhengxiang Huang[b,1], Xiao Ni[b], Chen Lv[b,*]

[a] Department of Orthopedics and Traumatology, the Affiliated Wenzhou Traditional Chinese Medicine Hospital, Zhejiang Chinese Medical University, Wenzhou 325000, Zhejiang, China
[b] Department of Orthopedics, the First Affiliated Hospital of Wenzhou Medical University, Wenzhou 325000, Zhejiang, China

ABSTRACT

Previous research has reported that piperlongumine exerts antitumor properties on several types of tumor cells. However, its effect on osteosarcoma cells remains unknown. This study aimed to investigate the antitumor effects of piperlongumine on osteosarcoma cells (MG63 and U2OS cells) in vitro and determined the underlying mechanism. Cell viability was measured using MTT assay. Cell apoptosis was assessed via AO/EB staining and flow cytometry apoptosis as well as western blot analysis. Cell cycle distribution was detected by flow cytometric cell cycle and western blot analysis. In our research, we found that piperlongumine induced apoptosis and G_2/M phase arrest of MG63 cells. Western blot analysis not only confirmed the above results, but also demonstrated that piperlongumine induced apoptosis of osteosarcoma cells by activating Caspase-9-dependent apoptotic pathway. Furthermore, we also found that piperlongumine significantly induced apoptosis and cell cycle arrest of osteosarcoma cells by regulating ROS/PI3K/Akt signaling pathway. In summary, our findings suggested that piperlongumine inhibited osteosarcoma progression by promoting apoptosis of osteosarcoma cells. In addition, the underlying mechanism demonstrated that piperlongumine produced potent antitumor properties in osteosarcoma cells by regulating ROS/PI3K/Akt signaling pathway

1. Introduction

Osteosarcoma (OS), one of the most common malignant bone tumor in the world, which accounts for 5% of pediatric tumor(Endo-Munoz et al., 2010), causes an extensive damage in children and adolescents (Chou et al., 2008). Due to abnormal division, unregulated proliferation and early metastasis, the 5-year survival rate of osteosarcoma is far from optimistic (Heymann et al., 2016). Epidemiological surveys demonstrated that pulmonary metastasis is the first leading cause of death of OS (Chang et al., 2015). With the improvement of surgical and neoadjuvant chemotherapy, the 5-year survival rate has increased to approximately 60% (Robl et al., 2015). Unfortunately, the long-term use of chemotherapy drugs has caused serious damage to normal tissues, especially liver and kidney (Bajpai et al., 2017; Villegas Rubio et al., 2017). Therefore, it is particularly important to find a safe and effective therapy drug for osteosarcoma.

Piperlongumine (PL), an alkaloid extracted from traditional Chinese medicine *Piper longum* L., has been reported to possess many

pharmacological effects including anti-inflammatory (Lee et al., 2013), anti-anxiety (anti-depression) (Cicero Bezerra Felipe et al., 2007), anti-platelet (Park et al., 2007), and anti-bacterial (Yang et al., 2002). Currently, more and more studies showed evidences that PL has antitumor properties in various tumor cells. For example, Duan et al. found that PL decreases gastric cancer cells apoptosis and G_2/M cell cycle arrest via suppressing STAT3 and TERT (Duan et al., 2016). Thongsom et al. demonstrated that PL induces human cholangiocarcinoma cells G_2/M phase arrest and apoptosis via suppressing ROS/JNK/ERK signaling pathway (Thongsom et al., 2017). Seok et al. reported that PL decreases human lung cancer cells proliferation and induces cell cycle arrest through inhibiting Akt pathway (Seok et al., 2018). The antiproliferative and apoptosis-inducing effects of PL were also reported in human breast cancer cells (Jin et al., 2017), human oral squamous cells (Chen et al., 2016b) and pancreatic cancer cells (Yamaguchi et al., 2018). In addition, PL was reported to have anti-invasive effect on human breast cancer cells (Liu et al., 2017). Although Aodah et al. earlier reported PL has a high cytotoxic activity on osteosarcoma cells,
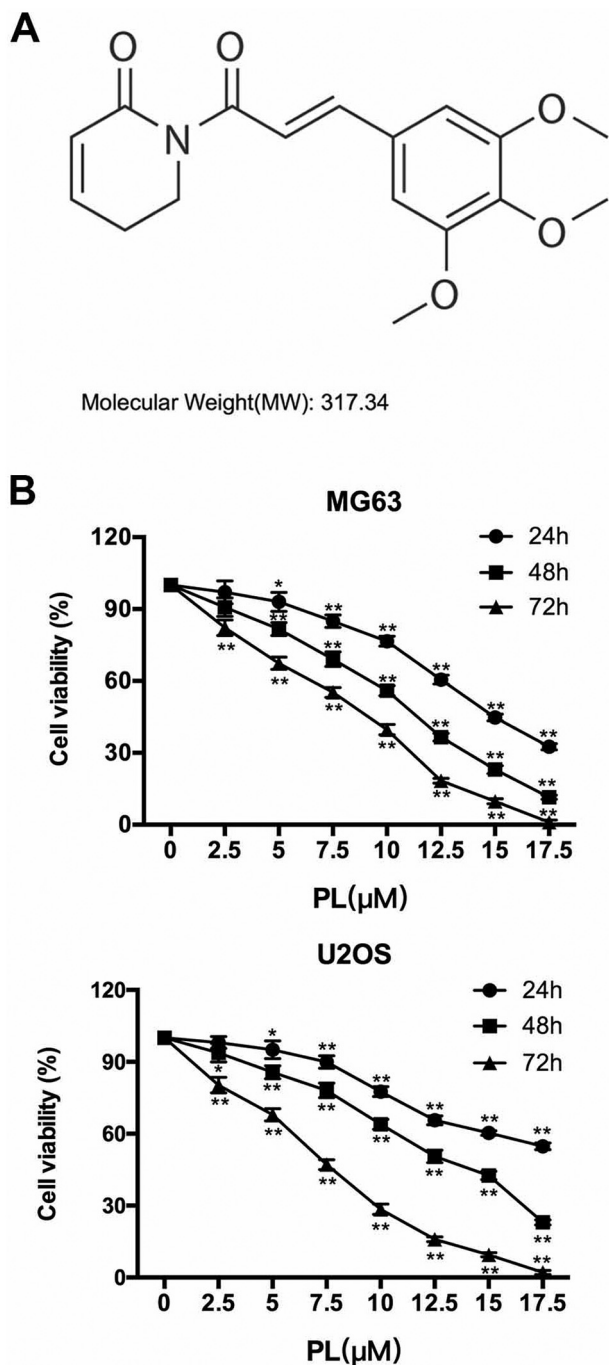
Fig. 1. PL suppresses osteosarcoma cells viability. (A) Molecular structure of PL. (B) The growth inhibitory effect was determined by MTT assay. MG63 and U2OS cells were treated with different concentrations (0 to 17.5 μM) of PL for 0 to 72 h. The growth inhibitory was in a time- and concentration-dependent manner. All statistical tests were based on the control group ($^*P < .05$, $^{**}P < .01$). Data are presented as the mean ± SEM of three independent experiments.

he only introduced it and did not elaborate on the mechanism of PL (Aodah et al., 2016). Therefore, the aims of our study were to evaluate the biological functions of PL on OS cells and explore the underlying mechanisms.

2. Materials and methods

2.1. Main reagents

Dulbecco's modified eagle medium (DMEM), fetal bovine serum (FBS), trypsin and penicillin/streptomycin were purchased from Gibco (Gaithersburg, MD, USA). Piperlongumine (PL, purity > 99%, molecular formula was shown in Fig. 1A) and LY294002 were purchased from Selleckchem (Houston, TX, USA). N-Acetyl-L-cysteine (NAC) was obtained from MedChemExpress (Monmouth, NJ, USA). Z-LEHD-FMK was purchased from ApexBio (Houston, TX, USA). 2,7′-Dichlorodihydrofluorescein diacetate (DCFH-DA) was obtained from Jiancheng (Nanjing, Jiangsu, China). Dimethyl sulfoxide (DMSO) and 3-(4,5-dimethyl-2-thiazolyl)-2,5-diphenyl-2-H-tetrazolium bromide (MTT) were purchased from Sigma (St. Louis, MO, USA). Annexin V-FITC/PI apoptosis detection kit and cell cycle detection kit were provided by Dojindo (Shanghai, China). Rabbit antibodies to Cyclin B1 (#12231, 1:1000), cdc2 (#28439, 1:1000), p21 (#2947, 1:1000), p53 (#2527, 1:1000), Cytochrome c (#4280, 1:1000), Caspase-3 (#9665, 1:1000), Caspase-7 (#9492, 1:1000), Caspase-9 (#9502, 1:1000), Bcl-2 (#4223, 1:1000), Bax (#5023, 1:1000), Akt (#4691, 1:1000) and p-Akt (#4060, 1:1000) were obtained from Cell Signaling Technology (Danvers, MA, USA). Rabbit antibody to GAPDH (sc-166,545, 1:5000), mouse antibody to β-Actin (sc-376,421, 1:5000), and horseradish peroxidase (HRP)-conjugated secondary antibodies (anti-rabbit, sc-2030, 1:5000; anti-mouse, sc-2031, 1:5000) were purchased from Santa Cruz Biotechnology (Santa Cruz, CA, USA). Enhanced chemiluminescence (ECL) western blot detection kit was provided by Beyotime (Shanghai, China).

2.2. Cell culture and treatments

Human osteosarcoma cell lines, MG63 and U2OS cells were purchased from ZQXZ Biotechnology (Shanghai, China). Cells were maintained in DMEM supplemented with 10% FBS and 1%penicillin/streptomycin at in a 37 °C humidified incubator containing 5% CO_2. Cells were treated with different concentration of PL in medium containing 10% FBS (PL was dissolved in DMSO before use). Pharmacological inhibitors such as Z-LEHD-FMK (50 μM, Caspase-9 specific inhibitor) (Chen et al., 2016a), NAC (5 mM, antioxidant, reduce ROS generation) (Wang et al., 2016)and LY294002 (20 μM, Akt specific inhibitor) (Jiang et al., 2014; Lv et al., 2017) were pretreated for 1 h before treatments of PL.

2.3. Cell viability assay

The viability of OS cells was evaluated by the MTT assay. Cells were incubated in 96-well plates for 24 h, then treated with different concentrations of PL (0 to 17.5 μM, 2.5 μM/gradient) for another 24, 48 and 72 h, each concentration for parallel 6 wells. After treatment, 10 μl MTT solution was added to each well. After incubating for 4 h, the medium was replaced with 150 μl DMSO solution to dissolve the precipitates (formazan crystals). The absorbance was read at a wavelength of 490 nm. Cell viability rate (%) = experimental group absorbance value/control group absorbance value × 100%. GraphPad Prism 6 software (GraphPad, San Diego, CA, USA) was used for calculation of half maximal inhibitory concentration (IC_{50}).

2.4. Morphological changes of apoptotic cells (Acridine orange/ethidium bromide (AO/EB) apoptosis assay)

Morphological changes of apoptotic osteosarcoma cells were observed directly using an inverted phase contrast. The two OS cells were treated with different concentrations of PL for 24 h. Then cells were observed directly under an inverted phase contrast microscope (100× magnification, Carl Zeiss, Heidenheimer, Germany). Next, we observed

the nuclear morphology of apoptotic cells using AO/EB staining. Cells were treated with different concentrations of PL (10 μM PL with or without Z-LEHD-FMK) for 24 h, washed twice with PBS, stained with 500 μl freshly-prepared dual stain solution containing 100 μg/ml AO and 100 μg/ml EB in the dark at room temperature for 5 min. The stained cells were observed using an inverted phase contrast fluorescence microscope (400× magnification, Carl Zeiss, Heidenheimer, Germany). The cells were counted from five random fields of each group, and the number of apoptotic cells was expressed as a percentage (%) of the total number of cells counted.

2.5. Measurement of intracellular ROS generation

Intracellular reactive oxygen species (ROS) generation of osteosarcoma cells was examined using the fluorescent probe DCFH-DA. In the presence of ROS, DCFH is oxidized to form a fluorescent substance, DCF. The intensity of green fluorescence is directly proportional to the level of intracellular ROS. The level of ROS in the cells can be known by detecting the fluorescence of DCF. Cells were treated with 10 μM PL (with or without NAC) for 24 h, detached by trypsin, centrifuged, washed twice with PBS, and incubated with 10 μM DCFH-DA at 37 °C for 30 min in the dark. The total level of ROS was observed under a laser scanning confocal microscope (400× magnification, Carl Zeiss, Heidenheimer, Germany) and measured by the changes in the mean fluorescence intensity (MFI) using Image J software (National Institutes of Health, Bethesda, MD, USA).

2.6. Flow cytometry cell apoptosis analysis

Flow cytometry cell apoptosis analysis was used to further confirm PL's role in cell apoptosis. Cells were treated with different concentrations of PL (with or without Z-LEHD-FMK, NAC, respectively) for 48 h, detached by trypsin, centrifuged, washed twice with PBS, resuspended in 500 μl binding buffer, and double stained with 5 μl Annexin V-FITC and 5 μl PI in the dark at room temperature for 15 min. The stained cells were measured using BD flow cytometer (FACSComp software, BD Biosciences, Franklin Lakes, NJ, USA). Annexin V-FITC$^+$/PI$^-$ cells were considered as early apoptotic cells, while Annexin V-FITC$^-$/PI$^+$ cells were considered as sum of late apoptotic cells and necrotic cells.

2.7. Flow cytometry cell cycle analysis

To observe the role of PL in cell cycle distribution, flow cytometry cell cycle analysis was measured. Cells were treated with different concentrations of PL for 24 h (with or without NAC). Following the treatments, cells were fixed in 70% ethanol at 4 °C overnight. Cells were washed with cold PBS, incubated with 100 μl RNase A at 37 °C for 30 min, and stained with 400 μl PI in the dark at room temperature for anther 30 min. The stained cells were measured using BD cytometer (CellQuest software, BD Biosciences, Franklin Lakes, NJ, USA).

2.8. Western blot analysis

To further confirm the molecular mechanism, western blot analysis was used. Cells (after treated with PL for 24 or 48 h) were collected by trypsin and lysed by RIPA lysis buffer. The lysates were centrifuged at 12,000 *g* at 4 °C for 20 min. The supernatants were collected and quantified. Protein samples were separated by SDS-PAGE and subsequently transferred to PVDF membranes. After transfer, the membranes were blocked with 5% nonfat milk in TBS-T at room temperature for 2 h, incubated with primary antibodies in TBS-T at 4 °C overnight, washed three times with TBS-T, and incubated with secondary antibodies in TBS-T at room temperature for 2 h. All proteins were detected using the ECL system. The density of the bands was analyzed using Image J software (National Institutes of Health, Bethesda, MD, USA) and normalized to house-keeping proteins (GAPDH or β-Actin).

2.9. Statistical analysis

All statistical analyses were performed with one-way ANOVA and Student-Newman-Keuls test using the SPSS 18.0 software (IBM, Armonk, NY, USA) and statistics charts were produced by GraphPad Prism 6 software (GraphPad, San Diego, CA, USA). Data were expressed as means ± standard error of the mean (SEM) and three independent experiments were analyzed. A probability value $P < .05$ was considered statistically significant.

3. Results

3.1. PL reduces cell viability of OS cells

Firstly, we investigated the growth inhibition of PL in OS cells using MTT assay. As shown in Fig. 1B, PL significantly inhibited cell viability of human OS cell lines MG63 and U2OS in a time- and concentration-dependent manner. Furthermore, the significantly growth inhibition ratio were both observed at 5 μM at 24 h, which similarly reached the maximum level at 17.5 μM at 72 h. The IC$_{50}$ (half maximal inhibitory concentration) value of PL to MG63 cells for 24, 48 and 72 h were 14.10, 9.97 and 7.24 μM, respectively ($^*P < .05$, $^{**}P < .01$, compared to control group), and the IC$_{50}$ value of PL to U2OS cells for 24, 48 and 72 h were 18.33, 12.32 and 6.56 μM, respectively ($^*P < .05$, $^{**}P < .01$, compared to control group). Based on our results, we chose 5, 10 (IC$_{50}$ approximately at 48 h) and 15 μM PL as the effective drug concentrations for the subsequent experiments throughout the study.

### 3.2. PL induces cell apoptosis of OS cells

Next, we compared the growth inhibitory effect after treatment with 5, 10 and 15 μM PL for 24 h. Morphological changes of both two OS cells were observed under an inverted phase contrast microscope. Cells in control group presented a long spindle or polygon appearance and attached uniformly to the culture dish. Nevertheless, some cells became small and round, and even suspended in medium in PL-treated groups. The number of non-adherent cells (dead cells) were significantly increased in PL-treated groups in a concentration-dependent manner, compared to control group ($^{**}P < .01$), respectively (Fig. 2A). Furthermore, we observed morphological changes of PL-treated MG63 cells using AO/EB staining assay under an inverted fluorescence microscope. The normal cell nucleus presented a green fluorescence, while the apoptotic cell nucleus showed a brighter green fluorescence and the structure became condensed. As shown in Fig. 2A, the percentage of apoptotic cell nuclei were significantly increased in PL-treated groups in a concentration-dependent manner, compared to control group ($^{**}P < .01$), respectively. Flow cytometry cell apoptosis assay was used to further confirm PL's role in inducing cell apoptosis in MG63 cells. The percentage of apoptotic cells was also significantly increased in PL-treated groups in a concentration-dependent manner, compared to control group ($^{**}P < .01$) (Fig. 3A). To investigate the molecular mechanism, we detected Bcl-2 and Caspase family proteins using western blot analysis. Cleaved Caspas-3 and Bax expression were significantly increased and Bcl-2 expression was significantly decreased in PL-treated groups in a concentration-dependent manner, compared to control group ($^*P < .05$, $^{**}P < .01$), respectively (Fig. 3B). The above results indicated that PL induced apoptosis of OS (MG63) cells in a concentration-dependent manner.

3.3. PL induces cell cycle arrest of OS cells

To investigate the effects of PL on cell cycle distribution, flow cytometry cell cycle assay was measured. As shown in Fig. 3C, PL significantly decreased the percentage of cells in G$_0$/G$_1$ and S phase, and increased the percentage of cells in G$_2$/M phase in a concentration-dependent manner, compared to control group ($^*P < .05$, $^{**}P < .01$).
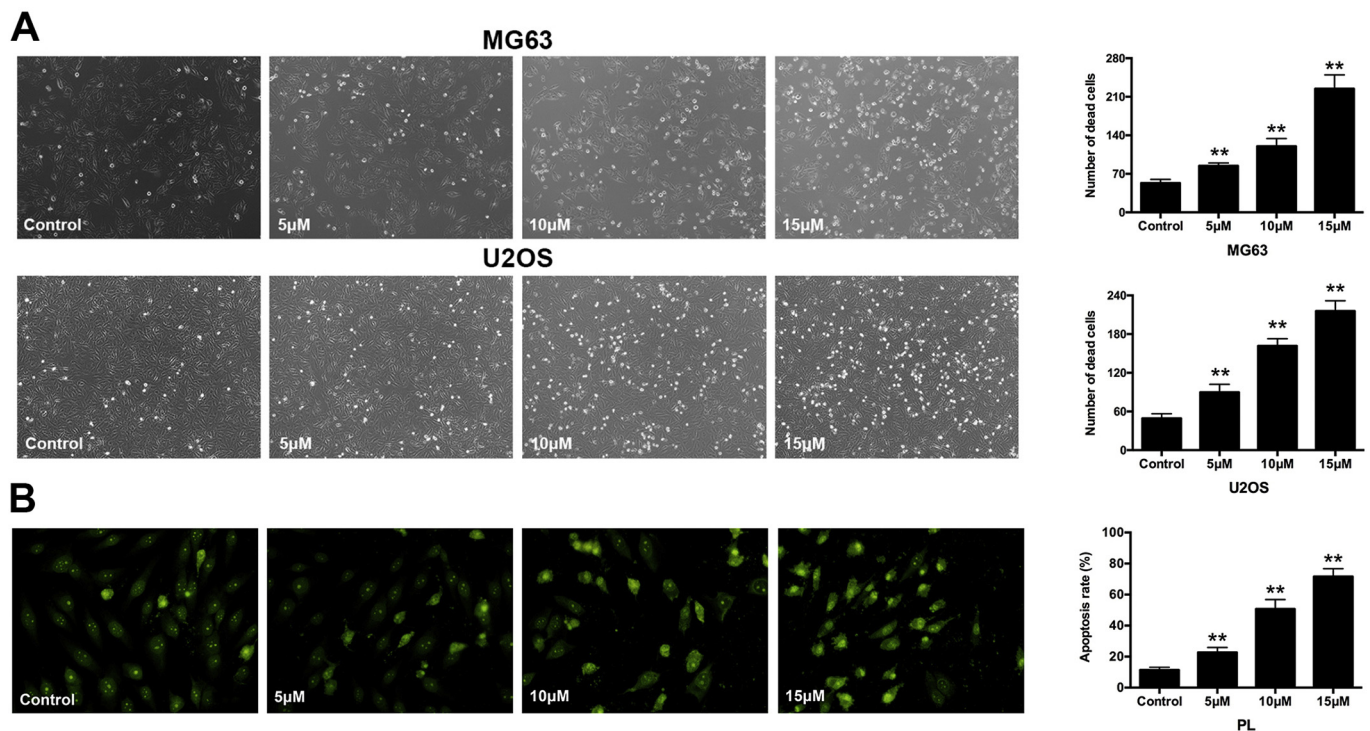
Fig. 2. Morphological appearance of osteosarcoma cells exposed to PL. (A) Morphological appearance of MG63 and U2OS cells exposed to 0 to 15 μM PL for 48 h was observed under an inverted phase-contrast microscope at 100 × magnification. The percentage of apoptotic cells were significantly increased in a concentration-dependent manner. (B) Nuclear morphological appearance of MG63 cells exposed to 0 to 15 μM PL for 48 h was observed under AO/EB staining and inverted phase-contrast microscope at 400 × magnification. The percentage of apoptotic nuclei were significantly increased in a concentration-dependent manner.

The results showed that PL induced G_2/M arrest in MG63 cells in a concentration-dependent manner. Moreover, to elucidate the molecular mechanism, we detected cell cycle related proteins expression (Cyclin B1, cdc2, p21 and p53) using western blot analysis. Cyclin B1 and cdc2 expression were significantly decreased and p21 and p53 expression were significantly increased in PL-treated groups in a concentration-dependent manner, compared to control group (*P < .05, **P < .01), respectively (Fig. 3D). The above results demonstrated that PL induced G_2/M arrest of MG63 cells in a concentration-dependent manner.

3.4. PL induces OS cells apoptosis via the Caspase-9-dependent apoptotic pathway

To evaluate whether Caspase-9 dependent apoptotic pathway was involved in PL-induced MG63 cells apoptosis, Z-LEHD-FMK, a Caspase-9 specific inhibitor, was used. In addition, we chose 10 μM PL for pretreatment. The apoptotic cell nucleus was significantly increased in PL-treated group, compared to control group (10 μM, **P < .01). This trend was blocked with the addition of Z-LEHD-FMK, compared to signal PL-treated group (10 μM, ##P < .01) (Fig. 4A). Similar trend was also observed in flow cytometry cell apoptosis assay (Fig. 4B). Next, we explore the molecular mechanism also using western blot analysis. As shown in Fig. 4C, the expression of Cleaved Caspase-3, Caspase-7 and Cleaved Caspase-9 were significantly increased in PL-treated group, compared to control group (**P < .01). However, the expressions of above proteins were significantly reduced in the presence of Z-LEHD-FMK, compared to signal PL-treated group (##P < .01). The results indicated that PL induced MG63 cells apoptosis via the Caspase-9-dependent apoptotic pathway.
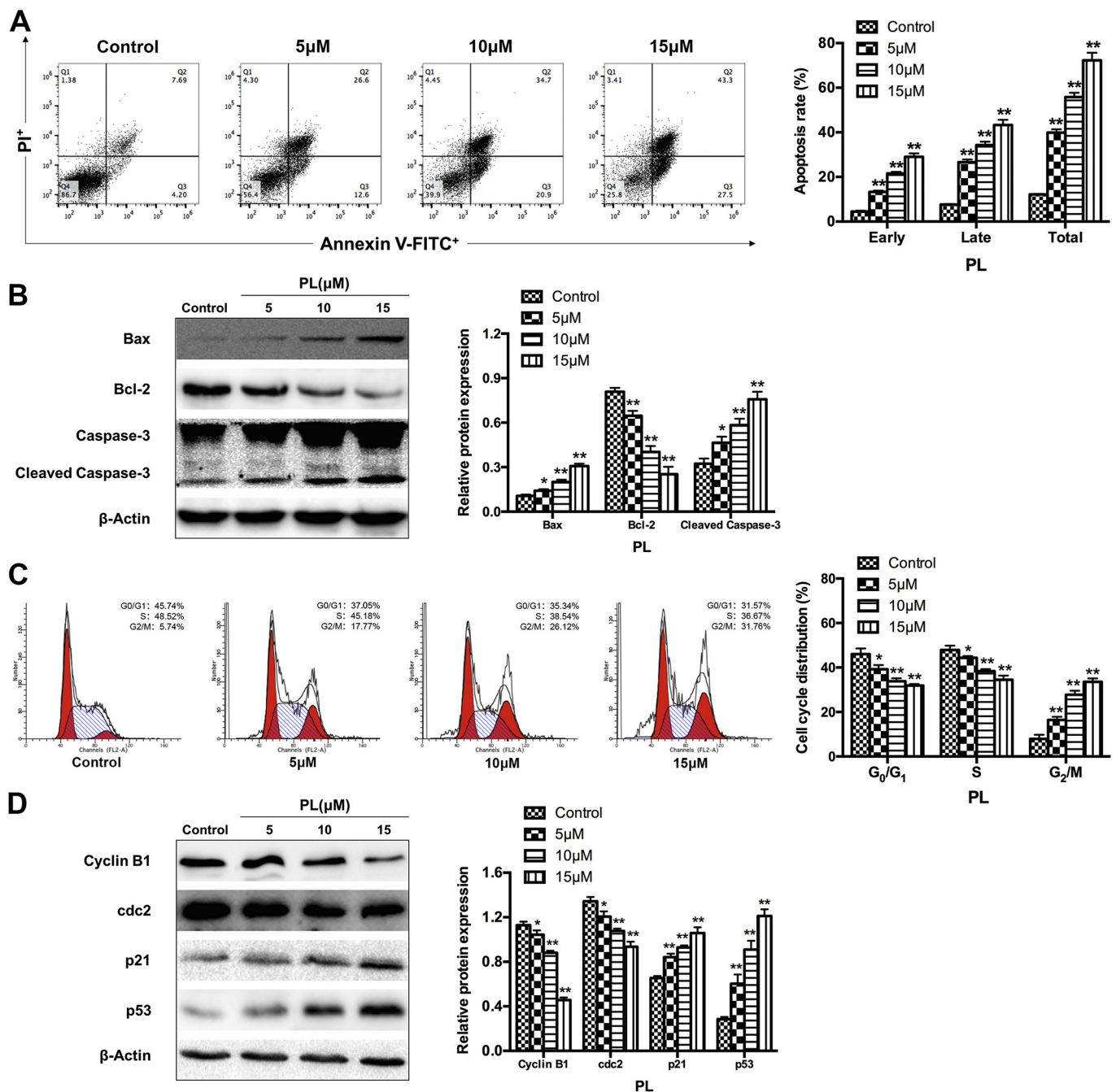
3.5. PL induces OS cells apoptosis and cell cycle arrest via ROS generation

Next, to evaluate whether PL induces MG63 cells apoptosis and cell cycle arrest via ROS generation, DCFH-DA fluorescent probe and NAC

(antioxidant) were used. In addition, we chose 10 μM PL for pretreatment. The intensity of green fluorescence (measured by Image J software) was significantly increased in PL-treated group, compared to control group (**P < .01). This trend was blocked with the addition of NAC, compared to signal PL-treated group (++P < .01) (Fig. 5A). Similar trend was also observed in flow cytometry cell apoptosis assay (NAC decreased PL induced cell apoptosis, ++P < .01) (Fig. 5B) and flow cytometry cell cycle assay (NAC decreased PL induced G_2/M arrest, 10 μM, +P < .05) (Fig. 5C). Next, we explored the molecular mechanism also using western blot analysis. As shown in Fig. 6A, the expression of pro-apoptosis proteins (Bax, Cytochrome c and Cleaved Caspase-3) were significantly increased and anti-apoptosis protein (Bcl-2) was significantly decreased in PL-treated group, compared to control group (**P < .01), respectively. However, the expressions of above proteins were significantly reversed in the presence of NAC, compared to signal PL-treated group (+P < .05, ++P < .01), respectively. As shown in Fig. 6B, the expression of cell cycle promotion proteins (G_2/M phase, Cyclin B1 and cdc2) were significantly decreased and cell cycle arrest proteins (G_2/M phase, p21 and p53) were significantly increased in PL-treated group, compared to control group (**P < .01), respectively, while the expression of above proteins were significantly reversed in the presence of NAC, compared to signal PL-treated group (+P < .05, ++P < .01). In conclusion, the above results indicated that PL induces MG63 cells apoptosis and G_2/M phase arrest via ROS generation.

3.6. PL inhibits PI3K/Akt signaling pathway in OS cells

To further investigate the mechanism of PL in inducing apoptosis and cell cycle arrest of MG63 cells, PI3K/Akt signaling pathway was analyzed. Western blot results showed that p-Akt was significantly decreased in PL groups in a concentration-dependent manner, compared to control group (**P < .01). Meanwhile, there was no significant difference in the expression of Akt in each group (Fig. 7A). Next, we

Fig. 3. PL induces apoptosis and cell cycle arrest of osteosarcoma cells. (A) Flow cytometry apoptosis was used to assess apoptosis of MG63 cells after treatment with PL (0 to 15 μM) for 48 h. PL significantly increased apoptosis in a concentration-dependent manner. (B) Western blot analysis was carried out to assess apoptosis related proteins expression in MG63 cells. β-Actin was used as an internal reference. PL significantly increased the expression of Bax and Cleaved Caspase-3 and decreased the expression of Bcl-2 in a concentration-dependent manner. (C) MG63 cells were treated with PL (0 to 15 μM) for 24 h and cell cycle distribution was analyzed by flow cytometry. PL significantly induced G_2/M phase arrest in a concentration-dependent manner. All statistical tests were based on the control group ($*P < .05$, $**P < .01$). Data are presented as the mean $\pm$ SEM of three independent experiments. (D) Western blot analysis was used to detect cell cycle related proteins expression in MG63 cells, β-Actin was used as an internal reference. PL significantly decreased the expression of Cyclin B1 and cdc2 and increased the expression of p21 and p53 in a concentration-dependent manner. All statistical tests were based on the control group ($*P < .05$, $**P < .01$). Data are presented as the mean $\pm$ SEM of three independent experiments.

investigated the effect of ROS on PI3K/Akt signaling pathway. The expression of p-Akt was significantly reversed in the presence of NAC, compared to signal PL-treated group ($^{++}P < .01$). There was also no significant difference in the expression of Akt in each group (Fig. 7B). Moreover, 20 μM of LY294002 (Wang et al., 2012), a specific inhibitor of Akt phosphorylation (activation), was used to further confirm the above hypothesis. As shown in Fig. 7C, p-Akt was significantly

decreased in PL + LY294002 group, compared to PL group ($^{\triangle\triangle}P < .01$). There was no significant change in the expression of Akt in each group. The above results were further confirmed by the comparison of (p-Akt/GAPDH)/(Akt/GAPDH) (Fig. 7A–C). Similarly, apoptosis and cell cycle related proteins were accordingly altered in PL + LY294002 group, compared to PL group ($^{\triangle}P < .05$, $^{\triangle\triangle}P < .01$), respectively (Fig. 7D and E). Taken together, the above
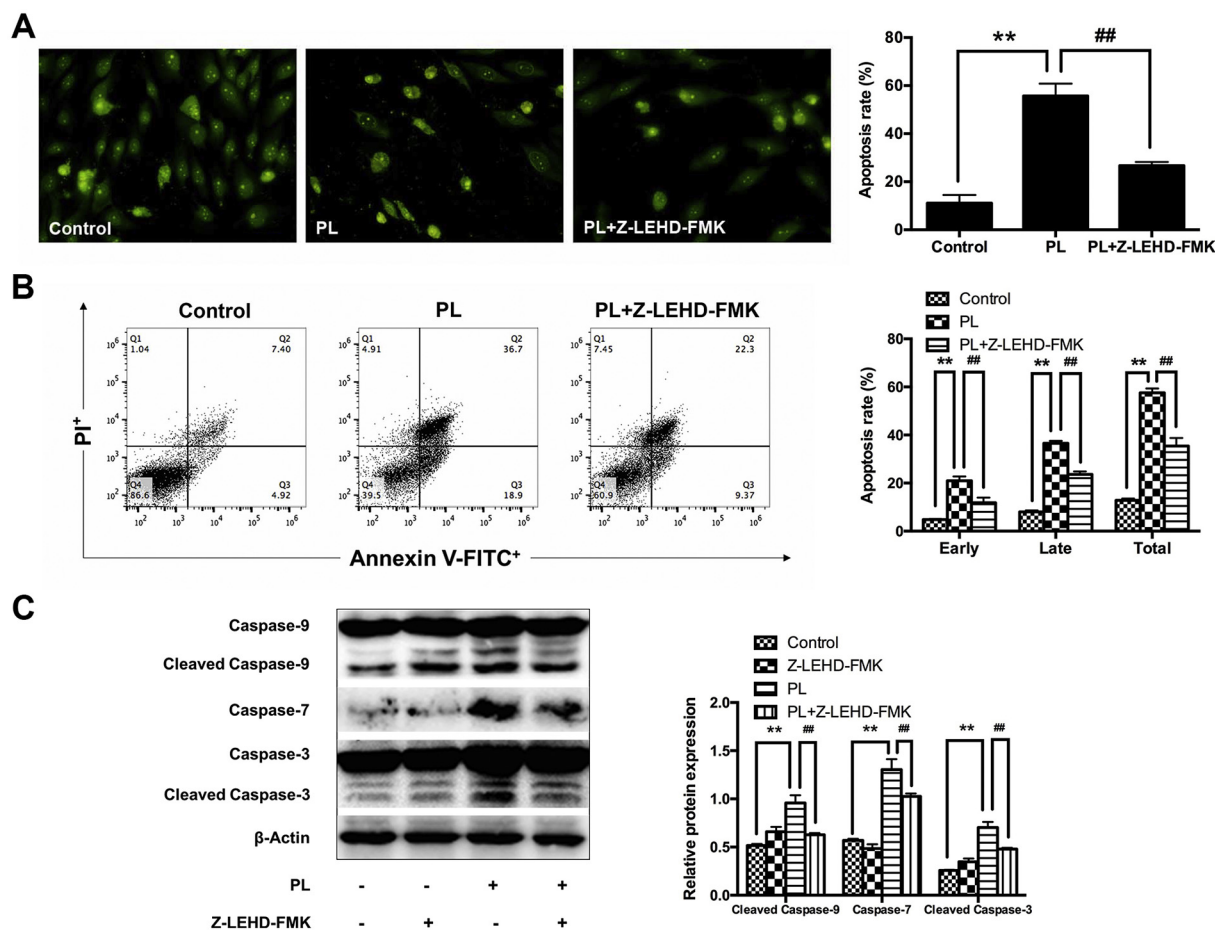
Fig. 4. PL induces apoptosis of MG63 cells via Caspase-9 dependent pathway. (A) Nuclear morphological appearance of MG63 cells exposed to PL with/without Z-LEHD-FMK for 48 h was observed under AO/EB staining and inverted phase-contrast microscope at 400× magnification. Z-LEHD-FMK significantly decreased the percentage of apoptotic nuclei in PL + Z-LEHD-FMK group, compared to PL group ($^{##}P < .01$). (B) Flow cytometry apoptosis was used to assess MG63 cells apoptosis after treatment with PL with/without Z-LEHD-FMK for 48 h. Z-LEHD-FMK significantly increased apoptosis rate of MG63 cells in PL + Z-LEHD-FMK group, compared to PL group ($^{##}P < .01$). (C) Western blot analysis was used to further confirm whether Caspase-9 independent pathway was involved in PL induced apoptosis of MG63 cells. β-Actin was used as an internal reference. PL significantly increased the expression of Cleaved Caspase-3, Caspase-7 and Cleaved Caspase-9 in PL group, compared to control group ($^{**}P < .01$). Z-LEHD-FMK significantly reversed the above related proteins expression in PL + Z-LEHD-FMK group, compared to PL group ($^{##}P < .01$). Data are presented as the mean ± SEM of three independent experiments.

results indicated that PI3K/Akt signaling pathway was involved in PL-induced apoptosis and cell cycle arrest in MG63 cells.

4. Discussion

In recent years, with the development of neoadjuvant chemotherapy, nearly 80% of patients can retain the affected limb and the metastasis rate and mortality of OS have been greatly reduced (Ji et al., 2013). However, there are still some patients who have poor chemotherapy effect are prone to relapse and metastasis. Therefore, it is urgent to find a novel therapeutic that can act effectively through various anticancer mechanisms. Traditional Chinese medicine has good anti-tumor effect, but due to its complex composition, unclear action mechanism, difficult quality control and toxic and side effects, which limits its extensive application in clinical practice (Hosoya et al., 2008). At present, in-depth study on active monomer compounds of traditional Chinese medicine will make up for these deficiencies and give full play to the anti-tumor activity of traditional Chinese medicine.

Among all of the effective components extracted from *Piper longum* L., PL exhibits powerful properties and has received notable attention (Bezerra et al., 2013). In recent years, research has shown that PL has selective targeting cytotoxic effects on tumor cells. PL has no significantly toxic and side effects on normal cells, tissues and organs, but

significantly inhibits tumor growth and metastasis (Raj et al., 2011). Therefore, we speculated that PL will become a hot topic of anti-tumor research in the near future, so as to develop effective drugs for tumor treatment. Studies have shown that PL can play an anti-tumor role by inducing various tumor cells apoptosis. However, to the best of our knowledge, the specific role and mechanism of PL in modulating OS were yet to be elucidated. Therefore, the current study aimed to clarify the role and mechanism of PL in modulating human osteosarcoma cells. The results of the present study showed that PL induces OS cells apoptosis via the Caspase-9-dependent apoptotic pathway. The underlying mechanisms of PL induces OS cells apoptosis and cell cycle arrest may be associated with the ROS/PI3K/Akt signaling pathway.

Uncontrolled cell proliferation is an important marker for tumor development. Therefore, to inhibit tumor cells growth or to promote tumor cells apoptosis is the most important objective to prevent tumor progression (Li et al., 2015a). In the present study, the effects of PL on cell apoptosis were examined in MG63 cells and MTT assay were performed. Our research proved that PL significantly inhibited MG63 cell viability in a time- and concentration-dependent manner. Results of cell morphological observation (AO/EB staining) and flow cytometric apoptosis detection (Annexin V/PI staining) further indicated that the decrease of MG63 cell viability in a time- and concentration-dependent manner induced by PL was associated with cell apoptosis. Then we
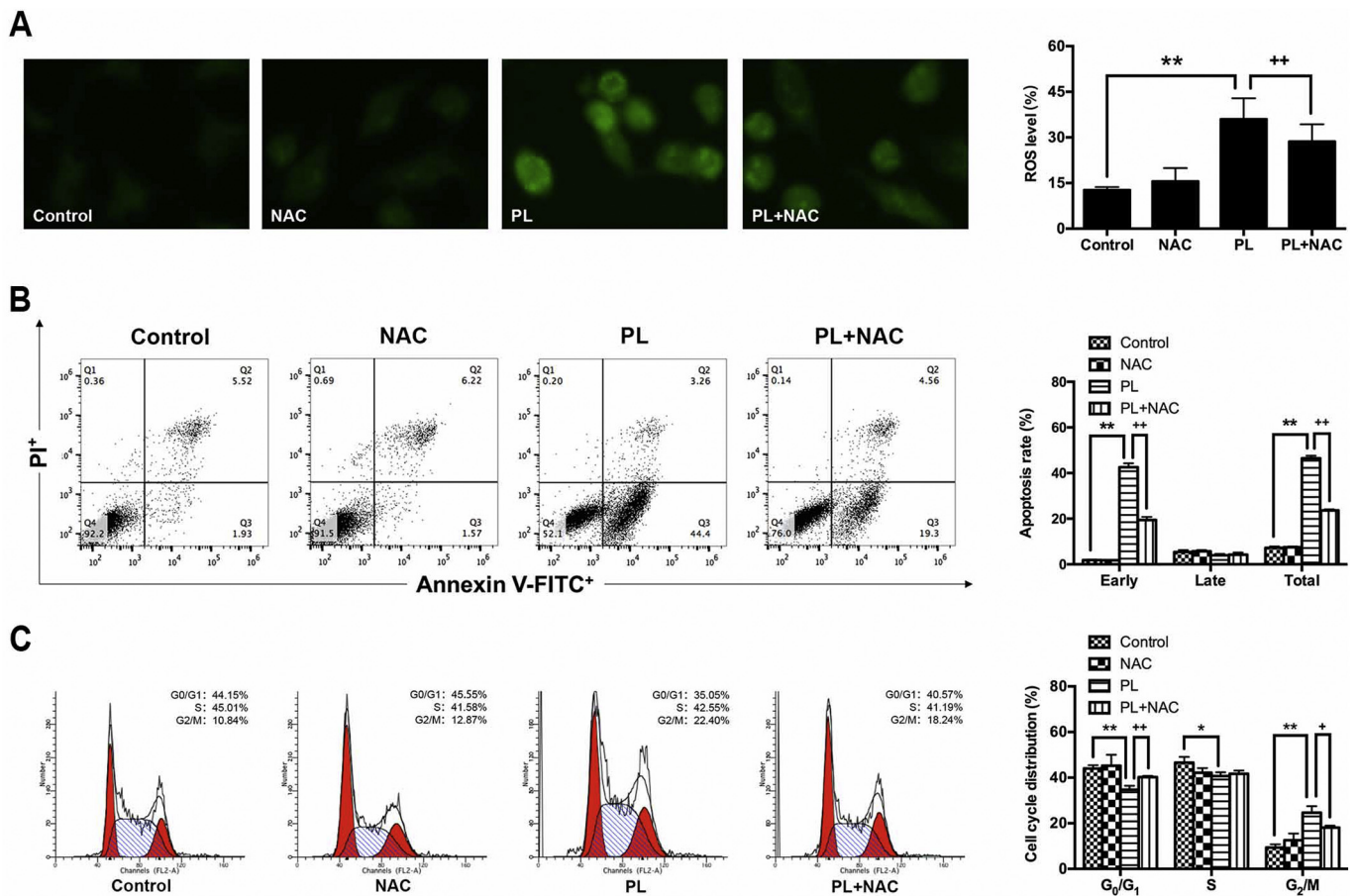
Fig. 5. PL induces apoptosis and cell cycle arrest of MG63 cells via ROS generation. (A) ROS generation after treatment with PL with/without NAC for 24 h was observed by DCFH-DA fluorescent probe and laser scanning confocal microscope at 400× magnification. Fluorescence intensity (ROS level) of MG63 cells was significantly increased in PL group, compared to control group (**P < .01). Meanwhile, NAC significantly decreased the increasing of PL-mediated ROS generation in PL + NAC group, compared to PL group (++P < .01). (B) Flow cytometry apoptosis was used to assess MG63 cells apoptosis after treatment with PL with/without NAC for 48 h. NAC significantly decreased apoptosis rate of MG63 cells in PL + NAC group, compared to PL group (++P < .01). (C) Consistent trend was detected by flow cytometry cell cycle. NAC significantly decreased G_2/M phase arrest in PL + NAC group, compared to PL group (+P < .05). Data are presented as the mean ± SEM of three independent experiments.

explored the apoptosis-associated proteins expression using western blot analysis. The expression levels of critical cell apoptosis, Bcl-2 and Caspase families, were regulated by PL, respectively.

Bcl-2 and Caspase families are the specific regulatory proteins of mitochondrial apoptosis pathway and are key regulators of apoptosis (Lv et al., 2016). Therefore, the present study results speculated that the mitochondrial apoptotic pathway was involved in PL-mediated apoptosis in MG63 cells. In addition, Dysregulated cell cycle distribution is another feature of tumor development, and induction of cell apoptosis is always together with cell cycle arrest (Gong et al., 2014). Through literature review, we found that the mechanism of PL in different tumor cells is not exactly the same. Several studies reported that PL induces G_0/G_1 phase cell cycle arrest in pancreatic ductal adenocarcinoma cells (Mohammad et al., 2018), lung cancer cells (Seok et al., 2018) and triple-negative breast cancer cells (Shrivastava et al., 2014). Other several studies showed that PL induces G_2/M phase cell cycle arrest in cholangiocarcinoma cells (Wang et al., 2012), colorectal cancer cells (Kumar and Agnihotri, 2019), melanoma cells (Song et al., 2018), gastric cancer cells (Duan et al., 2016), leukemia cells (Kang and Yan, 2015) and bladder cancer cells (Liu et al., 2017). However, the mechanism of PL in osteosarcoma cells has not been reported. So we evaluated the change of cell cycle distribution in osteosarcoma cells via flow cytometric cell cycle analysis (Lin et al., 2017). We found that PL triggered cell cycle arrest at G_2/M phase in MG63 cells in a concentration-dependent manner, which was consistent with previous

reports. Then we explored the cell cycle-related proteins expression also using western blot analysis. The expression levels of Cyclin B1, p21 and cdc2 were regulated by PL, respectively. Therefore, we concluded that the mitosis was gradually blocked followed the increasing concentrations of PL, which induces cell apoptosis of MG63 cells by inducing G_2/M phase arrest. Taken together, we suggested that PL may work as a cordial to induce cell apoptosis and G_2/M phase arrest in MG63 cells, and may represent as an alternative remedy for osteosarcoma.

Mitochondria, identified as a gatekeeper in the apoptotic pathway, plays a major role in cell apoptosis. Mitochondrial apoptotic pathway is one of the main pathways of apoptosis, and its mechanism is very complicated. Briefly, it refers to pro-apoptotic effectors regulates the expression of apoptosis-related proteins which lay on mitochondrial membrane (such as Bcl-2 family), increases the permeability of mitochondrial outer membrane, causes the release of apoptosis-related factors, activates Caspase-9 and Caspase-3, leads to cell apoptosis cascade reaction, and ultimately causes apoptosis. To further confirmed that PL induces apoptosis of MG63 cells through the mitochondrial apoptotic pathway, cell morphological observation and flow cytometric apoptosis detection were additionally measured. By AO/EB staining, we observed that cell apoptosis rate was significantly increased in PL-treated group, compared to control group. However, cell apoptosis rate was blocked upon the addition of Z-LEHD-FMK (Caspase-9 inhibitor). Results of Annexin V/PI staining also proved that cell apoptosis rate, both early and late-stage, were significantly increased in PL-treated
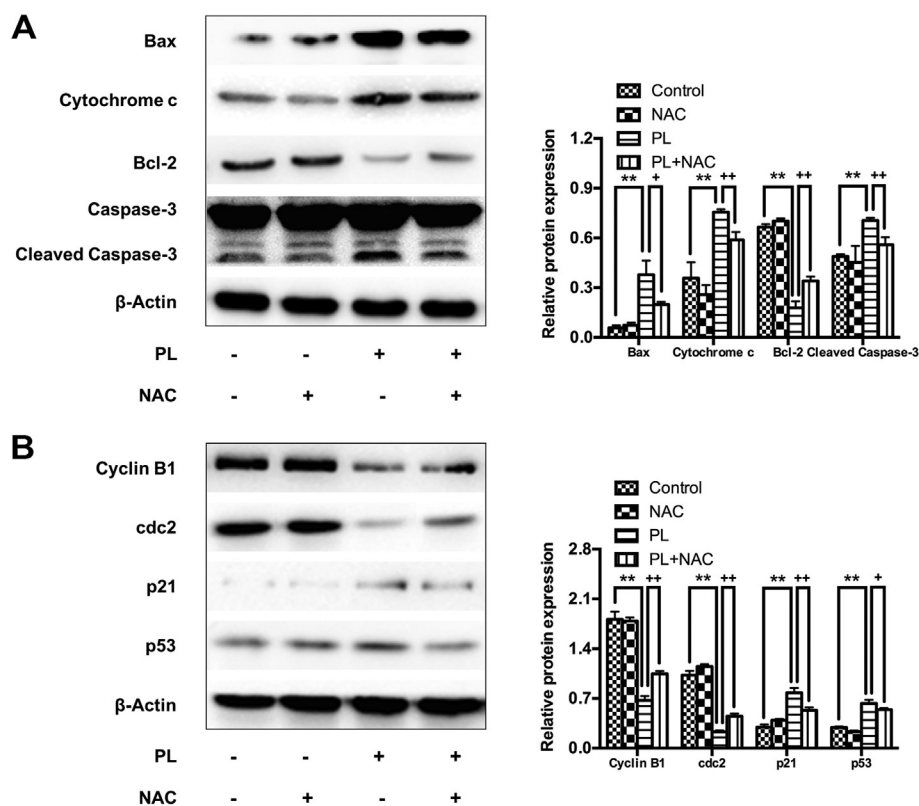
Fig. 6. Changes of apoptosis and cell cycle related proteins after treated with NAC. (A) Western blot analysis was carried out to assess apoptosis related proteins expression in MG63 cells. β-Actin was used as an internal reference. NAC significantly decreased the expression of Bax, Cytochrome c and Cleaved Caspase-3 and increased the expression of Bcl-2 in PL + NAC group, compared to PL group ($^+P < .05$, $^{++}P < .01$). (B) Western blot analysis was also used to detect cell cycle related proteins expression in MG63 cells, β-Actin was similarly used as an internal reference. NAC significantly increased the expression of Cyclin B1 and cdc2 and decreased the expression of p21 and p53 in in PL + NAC group, compared to PL group ($^+P < .05$, $^{++}P < .01$). Data are presented as the mean ± SEM of three independent experiments.

group compared to control group, but significantly blocked upon the addition of Z-LEHD-FMK. Combined with the above results, we implied that PL-induced cell apoptosis via the Caspase-9-dependent pathway. Caspase-9, an essential initiator caspase, is a primary caspase of the mitochondrial apoptotic pathway. Then we further confirmed the change of Caspase-3, 7, 9 proteins using western blot analysis. Consistent with previous results, the above Caspase proteins expressions were significantly increased PL-treated group compared to control group, but significantly blocked upon the addition of Z-LEHD-FMK. In summary, we demonstrated that PL induces MG63 cells apoptosis via the Caspase-9-dependent apoptotic pathway.

Abnormal cell metabolism produces a large amount of ROS, which exceeds the reductive capacity of the antioxidant system, and causes the cells to be in an oxidative stress state, which may cause changes in the expression of apoptosis-related genes and activate the apoptosis process. Previous studies reported that ROS generation plays a crucial role in the pro-apoptotic activities of various antitumor agents (Chao et al., 2017; Raj et al., 2011; Tu et al., 2016). Xiong et al. showed that PL induces apoptotic and autophagic death of the primary myeloid leukemia cells via activation of ROS (Xiong et al., 2015). Jin et al. reported that PL induces breast cancer cells death through ROS-mediated CHOP activation (Jin et al., 2014). Karki et al. proved that PL inhibits cell proliferation and induces apoptosis of pancreatic cancer cells via downregulating cMyc which mediated by ROS (Karki et al., 2017). Although previous studies have shown that PL can exert antitumor effects by activating ROS generation, whether its anti-tumor mechanism in different cells is consistent is unknown. Therefore, we investigated whether PL induced apoptosis of osteosarcoma cells was related to ROS generation. In our study, we used the fluorescent probe DCFH-DA to mark ROS generation and found that the ROS level in PL treated MG63 cells was significantly increased, while NAC (ROS inhibitor) significantly prevented the above changes. Meanwhile, the consistent results were found in flow cytometric cell apoptosis/cell cycle assays and western blot analysis which indicated that ROS generation is closely related to PL induced apoptosis and cycle arrest of MG63 cells.

By consulting literature, we found that the inhibition of PL on different tumor cells was related to different signaling pathways. Song et al. showed that PL inhibits gastric cancer cells proliferation, cell cycle progression and invasion via suppressing JAK1,2/STAT3 signaling pathway (Song et al., 2016). Zheng et al. proved that PL inhibits lung cancer cells growth via inhibiting NF-κB signaling pathway (Zheng et al., 2016). Wang et al. reported that PL induces leukemic cells apoptosis and autophagy by suppressing PI3K/Akt/mTOR signaling pathways and inducing p38 signaling pathways (Wang et al., 2018a). Li et al. is involved in PL induces human colorectal cancer cells apoptosis by activating JNK signaling pathway (Li et al., 2015b). In our study, we investigated the potential signaling pathway was involved in PL mediated-osteosarcoma cells apoptosis via western blot analysis. Interestingly, we found that the PI3K/Akt signaling pathway was participating in PL mediated MG63 cells apoptosis, which was consistent with other tumor cells mentioned in previous reports, such as human triple-negative breast cancer cells, human leukemic cells, and human lung cancer cells (Wang et al., 2015). Akt phosphorylation was decreased in a concentration-dependent manner. Researchers reported that PI3K/Akt signaling pathway is involved in the regulation of various biological processes, including cell survival, apoptosis, development and metastasis (Maddika et al., 2007; Zhou et al., 2015). Activating Akt (Akt phosphorylation) is considered as a key to promote tumor progression (Han et al., 2016). The over-activation of PI3K/Akt signaling pathway in many tumors is mainly due to the over activation of Akt (Yan-nan et al., 2014). Previous studies reported that ROS urges cell apoptosis by inhibiting PI3K/Akt pathway (Wang et al., 2018b; Xie et al., 2018). Our study results revealed that PL significantly inhibited Akt phosphorylation in MG63 cells while NAC prevented the inhibition of Akt phosphorylation, which suggested that ROS generation is a previous inhibition event of PI3K/Akt signaling pathway. Next, we used LY294002, a specific PI3K inhibitor, to further verified whether PI3K/Akt signaling pathway was involved in PL mediated MG63 cells apoptosis and G_2/M phase arrest. Western blot analysis results revealed that LY294002 not only enhanced the effect of PL in blocking the
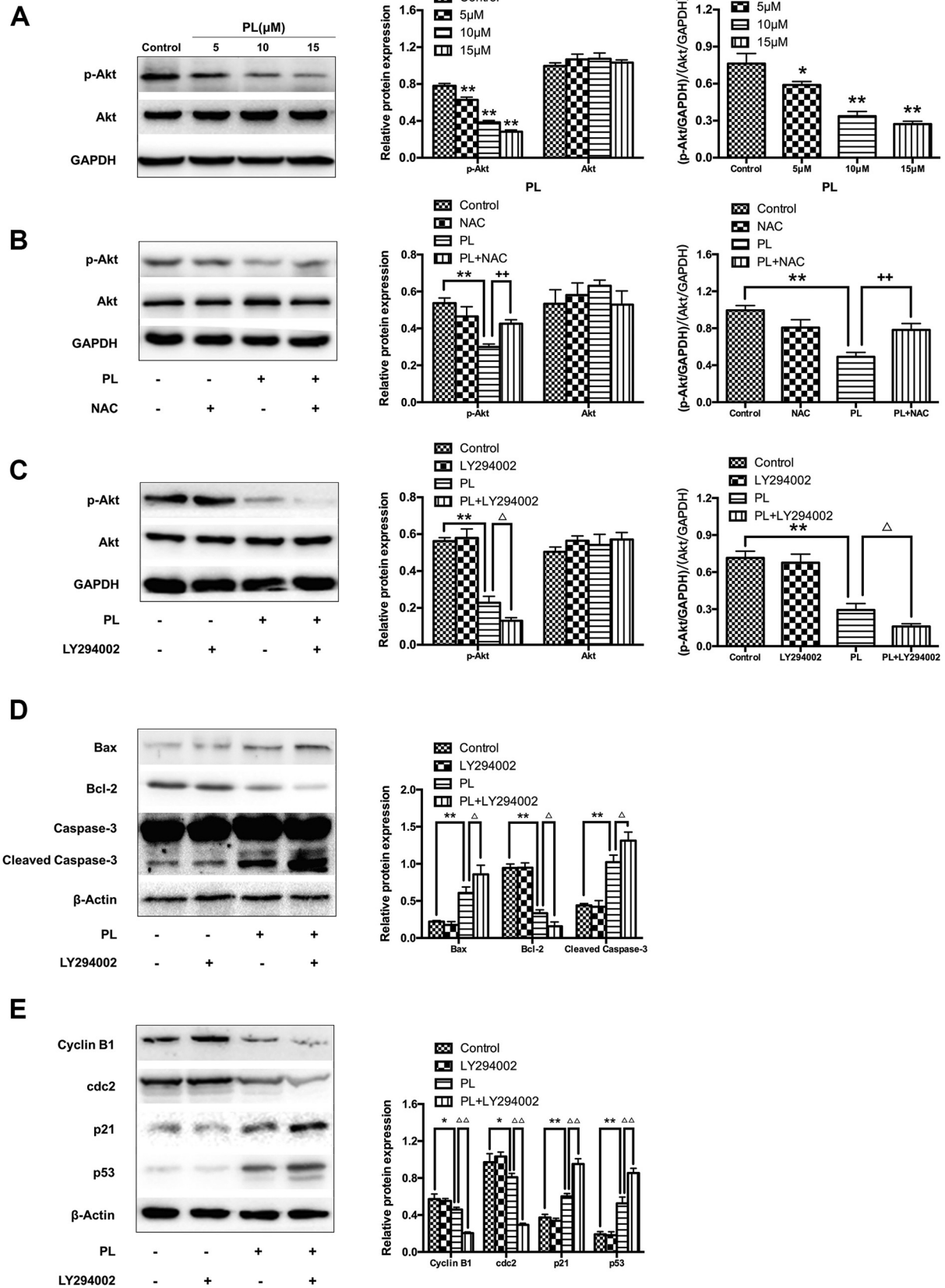
(caption on next page)

Fig. 7. PL induces apoptosis and cell cycle arrest of MG63 cells via inhibiting PI3K/Akt pathway. (A) Western blot analysis was used to speculate PL's effect on Akt phosphorylation. GAPDH was used as an internal reference. PL significantly inhibited Akt phosphorylation in a concentration-dependent manner, compared to control group ($^{**}P < .01$). (B) NAC was used to verify whether ROS was involved in regulation of Akt phosphorylation. GAPDH was used as an internal reference. NAC significantly increased Akt phosphorylation in PL + NAC group, compared to PL group ($^{++}P < .01$). (C) LY294002 was used to confirm PL's effect on Akt phosphorylation. GAPDH was used as an internal reference. LY294002 significantly enhanced the decreasing of PL-mediated Akt phosphorylation, compared to PL group ($^{\triangle}P < .05$). (D) LY294002 was used to measure whether PI3K/Akt pathway was involved in PL induced apoptosis of MG63 cells. Western blot analysis was used to assess apoptosis related proteins expression in MG63 cells. β-Actin was used as an internal reference. LY294002 significantly enhanced the increasing expression of Bax and Cleaved Caspase-3 and the decreasing expression of Bcl-2 in PL + NAC group, compared to PL group ($^{\triangle}P < .05$). (E) LY294002 and Western blot analysis was also used to measure whether PI3K/Akt pathway was involved in PL induced cell cycle arrest of MG63 cells. β-Actin was similarly used as an internal reference. Cyclin B1 and cdc2 and the increasing expression of p21 and p53 in in PL + NAC group, compared to PL group ($^{\triangle\triangle}P < .01$). Data are presented as the mean $\pm$ SEM of three independent experiments.
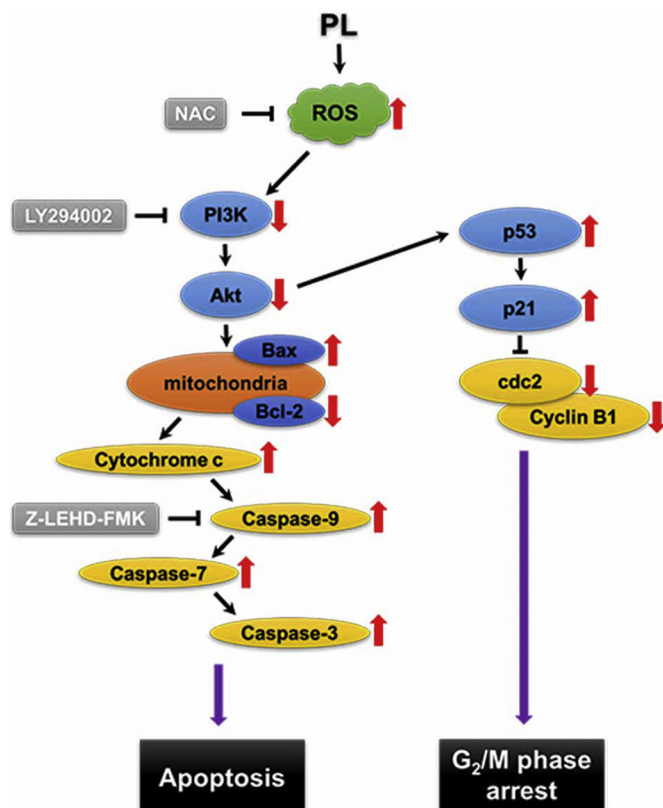
Fig. 8. Graphical abstract of the ROS/PI3K/Akt pathway involved in PL-induced apoptosis and cell cycle arrest (G₂/M phase) of osteosarcoma (MG63) cells.

phosphorylation of Akt, but also enhanced the effect of PL in promoting (blocking) the expression of pro-apoptotic (anti-apoptotic) and cell cycle arrest (cell cycle promotion) proteins, which indicated that PL induces cell apoptosis and cell cycle arrest in MG63 cells via ROS generation and inhibition of PI3K/Akt signaling pathway.

In this study, we demonstrated that PL as a critical inhibitor of osteosarcoma cells growth are associated with the induction of cell apoptosis and G₂/M phase arrest. Further mechanistic investigations suggested that activation of mitochondrial apoptosis pathway, ROS generation and inhibition of PI3K/Akt pathway could be the main mechanisms. In conclusion, our findings provided a basis molecular mechanism of PL in treating osteosarcoma (Fig. 8). The application of PL may provide a promising therapeutic strategy for osteosarcoma. Next, we will use more osteosarcoma cell lines and add the positive controls (p-Akt agonist) to verify our findings and make our study more convincing. Meanwhile, we will further clarify the pharmacological activity, action mechanism and safety of PL in animal models, so as to provide new and effective drugs for the clinical treatment of OS.

References

Aodah, A., Pavlik, A., Karlage, K., Myrdal, P.B., 2016. Preformulation studies on Piperlongumine. PLoS One 11, e0151707.

Bajpai, J., Chandrasekharan, A., Talreja, V., Simha, V., Chandrakanth, M.V., Rekhi, B., Khurana, S., Khan, A., Vora, T., Ghosh, J., Banavali, S.D., Gupta, S., 2017. Outcomes in non-metastatic treatment naive extremity osteosarcoma patients treated with a novel non-high dosemethotrexate-based, dose-dense combination chemotherapy regimen 'OGS-12. Eur. J. Cancer 85, 49–58.

Bezerra, D.P., Pessoa, C., de Moraes, M.O., Saker-Neto, N., Silveira, E.R., Costa-Lotufo, L.V., 2013. Overview of the therapeutic potential of piplartine (piperlongumine). Eur. J. Pharm. Sci. 48, 453–463.

Chang, L., Shrestha, S., LaChaud, G., Scott, M.A., James, A.W., 2015. Review of microRNA in osteosarcoma and chondrosarcoma. Med. Oncol. 32, 613.

Chao, C.C., Hou, S.M., Huang, C.C., Hou, C.H., Chen, P.C., Liu, J.F., 2017. Plumbagin induces apoptosis in human osteosarcoma through ROS generation, endoplasmic reticulum stress and mitochondrial apoptosis pathway. Mol. Med. Rep. 16, 5480–5488.

Chen, K., Ren, Q., Han, X.R., Zhang, X.N., Wei, B., Bai, X.Z., 2016a. Imatinib mesylate induces mitochondria-dependent apoptosis and inhibits invasion of human pigmented villonodular synovitis fibroblast-like synovial cells. Oncol. Rep. 35, 197–204.

Chen, S.Y., Liu, G.H., Chao, W.Y., Shi, C.S., Lin, C.Y., Lim, Y.P., Lu, C.H., Lai, P.Y., Chen, H.R., Lee, Y.R., 2016b. Piperlongumine suppresses proliferation of human Oral squamous cell carcinoma through cell cycle arrest, apoptosis and senescence. Int. J. Mol. Sci. 17.

Chou, A.J., Geller, D.S., Gorlick, R., 2008. Therapy for osteosarcoma: where do we go from here? Paediatr Drugs 10, 315–327.

Cicero Bezerra Felipe, F., Trajano Sousa Filho, J., de Oliveira Souza, L.E., Alexandre Silveira, J., Esdras de Andrade Uchoa, D., Rocha Silveira, E., Deusdenia Loiola Pessoa, O., de Barros Viana, G.S., 2007. Piplartine, an amide alkaloid from *Piper tuberculatum*, presents anxiolytic and antidepressant effects in mice. Phytomedicine 14, 605–612.

Duan, C., Zhang, B., Deng, C., Cao, Y., Zhou, F., Wu, L., Chen, M., Shen, S., Xu, G., Zhang, S., Duan, G., Yan, H., Zou, X., 2016. Piperlongumine induces gastric cancer cell apoptosis and G2/M cell cycle arrest both in vitro and in vivo. Tumour Biol. 37, 10793–10804.

Endo-Munoz, L., Cumming, A., Sommerville, S., Dickinson, I., Saunders, N.A., 2010. Osteosarcoma is characterised by reduced expression of markers of osteoclastogenesis and antigen presentation compared with normal bone. Br. J. Cancer 103, 73–81.

Gong, L.H., Chen, X.X., Wang, H., Jiang, Q.W., Pan, S.S., Qiu, J.G., Mei, X.L., Xue, Y.Q., Qin, W.M., Zheng, F.Y., Shi, Z., Yan, X.J., 2014. Piperlongumine induces apoptosis and synergizes with cisplatin or paclitaxel in human ovarian cancer cells. Oxidative Med. Cell. Longev. 2014, 906804.

Han, L., Liu, B., Jiang, L., Liu, J., Han, S., 2016. MicroRNA-497 downregulation contributes to cell proliferation, migration, and invasion of estrogen receptor alpha negative breast cancer by targeting estrogen-related receptor alpha. Tumour Biol. 37, 13205–13214.

Heymann, M.F., Brown, H.K., Heymann, D., 2016. Drugs in early clinical development for the treatment of osteosarcoma. Expert Opin. Investig. Drugs 25, 1265–1280.

Hosoya, K., Murahari, S., Laio, A., London, C.A., Couto, C.G., Kisseberth, W.C., 2008.

Biological activity of dihydroartemisinin in canine osteosarcoma cell lines. Am. J. Vet. Res. 69, 519–526.

Ji, F., Zhang, H., Wang, Y., Li, M., Xu, W., Kang, Y., Wang, Z., Wang, Z., Cheng, P., Tong, D., Li, C., Tang, H., 2013. MicroRNA-133a, downregulated in osteosarcoma, suppresses proliferation and promotes apoptosis by targeting Bcl-xL and Mcl-1. Bone 56, 220–226.

Jiang, X., Tang, X., Zhang, P., Liu, G., Guo, H., 2014. Cyanidin-3-O-beta-glucoside protects primary mouse hepatocytes against high glucose-induced apoptosis by modulating mitochondrial dysfunction and the PI3K/Akt pathway. Biochem. Pharmacol. 90, 135–144.

Jin, H.O., Lee, Y.H., Park, J.A., Lee, H.N., Kim, J.H., Kim, J.Y., Kim, B., Hong, S.E., Kim, H.A., Kim, E.K., Noh, W.C., Kim, J.I., Chang, Y.H., Hong, S.I., Hong, Y.J., Park, I.C., Lee, J.K., 2014. Piperlongumine induces cell death through ROS-mediated CHOP activation and potentiates TRAIL-induced cell death in breast cancer cells. J. Cancer Res. Clin. Oncol. 140, 2039–2046.

Jin, H.O., Park, J.A., Kim, H.A., Chang, Y.H., Hong, Y.J., Park, I.C., Lee, J.K., 2017. Piperlongumine downregulates the expression of HER family in breast cancer cells. Biochem. Biophys. Res. Commun. 486, 1083–1089.

Kang, Q., Yan, S., 2015. Piperlongumine reverses doxorubicin resistance through the PI3K/Akt signaling pathway in K562/A02 human leukemia cells. Exp Ther Med 9, 1345–1350.

Karki, K., Hedrick, E., Kasiappan, R., Jin, U.H., Safe, S., 2017. Piperlongumine induces reactive oxygen species (ROS)-dependent Downregulation of specificity protein transcription factors. Cancer Prev. Res. (Phila.) 10, 467–477.

Kumar, S., Agnihotri, N., 2019. Piperlongumine, a piper alkaloid targets Ras/PI3K/Akt/ mTOR signaling axis to inhibit tumor cell growth and proliferation in DMH/DSS induced experimental colon cancer. Biomed. Pharmacother. 109, 1462–1477.

Lee, W., Yoo, H., Kim, J.A., Lee, S., Jee, J.G., Lee, M.Y., Lee, Y.M., Bae, J.S., 2013. Barrier protective effects of piperlonguminine in LPS-induced inflammation in vitro and in vivo. Food Chem. Toxicol. 58, 149–157.

Li, J., Sharkey, C.C., King, M.R., 2015a. Piperlongumine and immune cytokine TRAIL synergize to promote tumor death. Sci. Rep. 5, 9987.

Li, W., Wen, C., Bai, H., Wang, X., Zhang, X., Huang, L., Yang, X., Iwamoto, A., Liu, H., 2015b. JNK signaling pathway is involved in piperlongumine-mediated apoptosis in human colorectal cancer HCT116 cells. Oncol. Lett. 10, 709–715.

Lin, W., Zhu, X., Yang, S., Chen, X., Wang, L., Huang, Z., Ding, Y., Huang, L., Lv, C., 2017. MicroRNA-203 inhibits proliferation and invasion, and promotes apoptosis of osteosarcoma cells by targeting runt-related transcription factor 2. Biomed. Pharmacother. 91, 1075–1084.

Liu, D., Qiu, X.Y., Wu, X., Hu, D.X., Li, C.Y., Yu, S.B., Pan, F., Chen, X.Q., 2017. Piperlongumine suppresses bladder cancer invasion via inhibiting epithelial mesenchymal transition and F-actin reorganization. Biochem. Biophys. Res. Commun. 494, 165–172.

Lv, C., Hao, Y., Han, Y., Zhang, W., Cong, L., Shi, Y., Tu, G., 2016. Role and mechanism of microRNA-21 in H2O2-induced apoptosis in bone marrow mesenchymal stem cells. J. Clin. Neurosci. 27, 154–160.

Lv, C., Yang, S., Chen, X., Zhu, X., Lin, W., Wang, L., Huang, Z., Wang, M., Tu, G., 2017. MicroRNA-21 promotes bone mesenchymal stem cells migration in vitro by activating PI3K/Akt/MMPs pathway. J. Clin. Neurosci. 46, 156–162.

Maddika, S., Ande, S.R., Panigrahi, S., Paranjothy, T., Weglarczyk, K., Zuse, A., Eshraghi, M., Manda, K.D., Wiechec, E., Los, M., 2007. Cell survival, cell death and cell cycle pathways are interconnected: implications for cancer therapy. Drug Resist. Updat. 10, 13–29.

Mohammad, J., Dhillon, H., Chikara, S., Mamidi, S., Sreedasyam, A., Chittem, K., Orr, M., Wilkinson, J.C., Reindl, K.M., 2018. Piperlongumine potentiates the effects of gemcitabine in in vitro and in vivo human pancreatic cancer models. Oncotarget 9, 10457–10469.

Park, B.S., Son, D.J., Park, Y.H., Kim, T.W., Lee, S.E., 2007. Antiplatelet effects of acidamides isolated from the fruits of Piper longum L. Phytomedicine 14, 853–855.

Raj, L., Ide, T., Gurkar, A.U., Foley, M., Schenone, M., Li, X., Tolliday, N.J., Golub, T.R., Carr, S.A., Shamji, A.F., Stern, A.M., Mandinova, A., Schreiber, S.L., Lee, S.W., 2011. Selective killing of cancer cells by a small molecule targeting the stress response to ROS. Nature 475, 231–234.

Robl, B., Pauli, C., Botter, S.M., Bode-Lesniewska, B., Fuchs, B., 2015. Prognostic value of

tumor suppressors in osteosarcoma before and after neoadjuvant chemotherapy. BMC Cancer 15, 379.

Seok, J.S., Jeong, C.H., Petriello, M.C., Seo, H.G., Yoo, H., Hong, K., Han, S.G., 2018. Piperlongumine decreases cell proliferation and the expression of cell cycle-associated proteins by inhibiting Akt pathway in human lung cancer cells. Food Chem. Toxicol. 111, 9–18.

Shrivastava, S., Kulkarni, P., Thummuri, D., Jeengar, M.K., Naidu, V.G., Alvala, M., Reddy, G.B., Ramakrishna, S., 2014. Piperlongumine, an alkaloid causes inhibition of PI3 K/Akt/mTOR signaling axis to induce caspase-dependent apoptosis in human triple-negative breast cancer cells. Apoptosis 19, 1148–1164.

Song, B., Zhan, H., Bian, Q., Gu, J., 2016. Piperlongumine inhibits gastric cancer cells via suppression of the JAK1,2/STAT3 signaling pathway. Mol. Med. Rep. 13, 4475–4480.

Song, X., Gao, T., Lei, Q., Zhang, L., Yao, Y., Xiong, J., 2018. Piperlongumine induces apoptosis in human melanoma cells via reactive oxygen species mediated mitochondria disruption. Nutr. Cancer 70, 502–511.

Thongsom, S., Suginta, W., Lee, K.J., Choe, H., Talabnin, C., 2017. Piperlongumine induces G2/M phase arrest and apoptosis in cholangiocarcinoma cells through the ROS-JNK-ERK signaling pathway. Apoptosis 22, 1473–1484.

Tu, P., Huang, Q., Ou, Y., Du, X., Li, K., Tao, Y., Yin, H., 2016. Aloe-emodin-mediated photodynamic therapy induces autophagy and apoptosis in human osteosarcoma cell line MG63 through the ROS/JNK signaling pathway. Oncol. Rep. 35, 3209–3215.

Villegas Rubio, J.A., Cacciavillano, W., Rose, A., Zubizarreta, P., Scopinaro, M., 2017. Ambulatory high-dose methotrexate Administration in Pediatric Osteosarcoma Patients at a single institution in Argentina. J. Pediatr. Hematol. Oncol. 39, e349–e352.

Wang, H., Zhang, Q., Zhang, L., Little, P.J., Xie, X., Meng, Q., Ren, Y., Zhou, L., Gao, G., Quirion, R., Zheng, W., 2012. Insulin-like growth factor-1 induces the phosphorylation of PRAS40 via the PI3K/Akt signaling pathway in PC12 cells. Neurosci. Lett. 516, 105–109.

Wang, F., Mao, Y., You, Q., Hua, D., Cai, D., 2015. Piperlongumine induces apoptosis and autophagy in human lung cancer cells through inhibition of PI3K/Akt/mTOR pathway. Int. J. Immunopathol. Pharmacol. 28, 362–373.

Wang, H., Sun, N., Li, X., Li, K., Tian, J., Li, J., 2016. Diallyl trisulfide induces osteosarcoma cell apoptosis through reactive oxygen species-mediated downregulation of the PI3K/Akt pathway. Oncol. Rep. 35, 3648–3658.

Wang, H., Wang, Y., Gao, H., Wang, B., Dou, L., Li, Y., 2018a. Piperlongumine induces apoptosis and autophagy in leukemic cells through targeting the PI3K/Akt/mTOR and p38 signaling pathways. Oncol. Lett. 15, 1423–1428.

Wang, S.W., Deng, L.X., Chen, H.Y., Su, Z.Q., Ye, S.L., Xu, W.Y., 2018b. MiR-124 affects the apoptosis of brain vascular endothelial cells and ROS production through regulating PI3K/AKT signaling pathway. Eur. Rev. Med. Pharmacol. Sci. 22, 498–505.

Xie, C., Yi, J., Lu, J., Nie, M., Huang, M., Rong, J., Zhu, Z., Chen, J., Zhou, X., Li, B., Chen, H., Lu, N., Shu, X., 2018. N-Acetylcysteine reduces ROS-mediated oxidative DNA damage and PI3K/Akt pathway activation induced by helicobacter pylori infection. Oxidative Med. Cell. Longev. 2018, 1874985.

Xiong, X.X., Liu, J.M., Qiu, X.Y., Pan, F., Yu, S.B., Chen, X.Q., 2015. Piperlongumine induces apoptotic and autophagic death of the primary myeloid leukemia cells from patients via activation of ROS-p38/JNK pathways. Acta Pharmacol. Sin. 36, 362–374.

Yamaguchi, Y., Kasukabe, T., Kumakura, S., 2018. Piperlongumine rapidly induces the death of human pancreatic cancer cells mainly through the induction of ferroptosis. Int. J. Oncol. 52, 1011–1022.

Yang, Y.C., Lee, S.G., Lee, H.K., Kim, M.K., Lee, S.H., Lee, H.S., 2002. A piperidine amide extracted from Piper longum L. fruit shows activity against Aedes aegypti mosquito larvae. J. Agric. Food Chem. 50, 3765–3767.

Yan-nan, B., Zhao-yan, Y., Li-xi, L., jiang, Y., Qing-jie, X., Yong, Z., 2014. MicroRNA-21 accelerates hepatocyte proliferation in vitro via PI3K/Akt signaling by targeting PTEN. Biochem. Biophys. Res. Commun. 443, 802–807.

Zheng, J., Son, D.J., Gu, S.M., Woo, J.R., Ham, Y.W., Lee, H.P., Kim, W.J., Jung, J.K., Hong, J.T., 2016. Piperlongumine inhibits lung tumor growth via inhibition of nuclear factor kappa B signaling pathway. Sci. Rep. 6, 26357.

Zhou, Z.W., Li, X.X., He, Z.X., Pan, S.T., Yang, Y., Zhang, X., Chow, K., Yang, T., Qiu, J.X., Zhou, Q., Tan, J., Wang, D., Zhou, S.F., 2015. Induction of apoptosis and autophagy via sirtuin1- and PI3K/Akt/mTOR-mediated pathways by plumbagin in human prostate cancer cells. Drug Des Devel Ther 9, 1511–1554.